J2.7 PREDICTING DROUGHT VULNERABILITY IN THE MEDITERRANEAN

J. P. Palutikof and T. Holt
Climatic Research Unit, University of East Anglia, Norwich, UK

1. INTRODUCTION

Mediterranean water resources are under severe stress. Rainfall amounts barely meet demand, and there is competition between agriculture and tourism in summer, with a high water requirement coinciding with low to zero rainfall amounts. The situation is dynamic, and unlikely to improve in the future. The current resident population in the countries bordering the Mediterranean Sea is 450 million (in 1997) and is projected to increase to 520-570 million in 2030. Tourism to the Mediterranean region was estimated at 135 million visits in 1990 and is projected to increase to as many as 235-350 million visits in 2025 (European Environment Agency, 2001).

In the face of this rapidly-evolving situation, there is a need to understand the impact that anthropogenic climate change may have on future water resources. We use climate model output to examine the effect of climate change on water resources in the Mediterranean region. The work is based on the Hadley Centre regional climate model HadRM3 (Hulme et al., 2002).

We take two approaches, based on:

- the balance between rainfall and evapotranspiration, from which a measure of moisture availability can be calculated.
- indices of daily precipitation which provide insights into the behavior of the precipitation regime, particularly at the extremes. The indices used here are:
    - Maximum length of dry spell
    - Start of the summer dry period
    - End of the summer dry period
    - The maximum 5-day running sum of rainfall in a year.

2. MODEL CHARACTERISTICS

HADRM3 has a spatial resolution of about 50 km (0.44^o by 0.44^o). The domain is the European region. The boundary conditions are taken from HadAM3, which is an atmosphere-only global model run as an intermediate step in dynamical downscaling between HadCM3 (which has a resolution of 2.5° latitude by 3.75° longitude) and HadRM3, with a resolution four times that of HadCM3. The regional model was run for two time slices: a 1961-90 control period, and A2 and B2 SRES scenarios for 2070-2100. There are three ensemble members for the control period and A2 scenario (*a*, *b* and *c*) and one simulation for B2, based on B2a from HadCM3. We have available a standard set of surface variables for the control and A2 ensembles a, b and c, and for B2a.

Corresponding author address: Jean Palutikof, Climatic Research Unit, University of East Anglia, Norwich NR4 7TJ, UK; e-mail: j.palutikof@uea.ac.uk

3. MOISTURE AVAILABILITY

Both rainfall and temperature are expected to change in response to global warming. The impacts of these changes will not be due simply to the change in their separate behaviour, but also as a response to their interactions. The goal was to find a relatively simple measure which would express the interactions between temperature and precipitation, so that changes in this measure in response to the enhanced greenhouse effect could be explored. This requires that both the variable expressing precipitation and the variable expressing temperature should be measured in the same units. By transforming temperature into a measure of potential evapotranspiration, we can achieve this goal, and then work towards defining a measure expressing the relationship between precipitation and potential evapotranspiration, both measured as a depth. This measure we term the *index of moisture availability* (IMA).

The IMA is derived from the balance between precipitation (P) and potential evapotranspiiration (Et), using monthly data. We explored the use of a ratio, P/Et, and of a difference, P – Et. We found that the spatial variations across the Mediterranean region in the ratio were extremely large, especially in the summer season, making it impossible to produce meaningful contoured maps. The IMA is therefore defined as the difference, P – Et, in mm.

3.1 Calculating potential evapotranspiration

In an earlier paper (Palutikof et al., 1994), we explored a number of algorithms to calculate potential evapotranspiration. The goal was to find a simple measure, based primarily around temperature. In validating the techniques, we used Penman Et as the standard against which the simpler methods could be compared. We found, for example, that the Thornthwaite method gave values of Et in the Mediterranean region which were generally too low.

More accurate results were obtained using the Blaney and Criddle method. The original Blaney and Criddle (1977) method used only temperature, t, and day length, d, to derive a consumptive use factor, f:

$$f = d[(1.8t + 32)/100]$$

This method was modified by Doorenbos and Pruitt (1977) to calculate evapotranspiration directly from:

$$Et = c[d(0.46t + 8)]$$

where c is an adjustment factor. Palutikof et al. (1994) developed seasonal transfer functions to calculate the adjustment factor, c, using only temperature as the predictor variable.

3.2 Calculating the IMA

Following the calculation of Et, the IMA is found by performing the simple subtraction P – Et. All calculations were performed at the monthly level, and the results averaged to give seasonal means for the periods 1961-90 and 2070-2100, which could be compared. The procedure is shown in Figure 1.

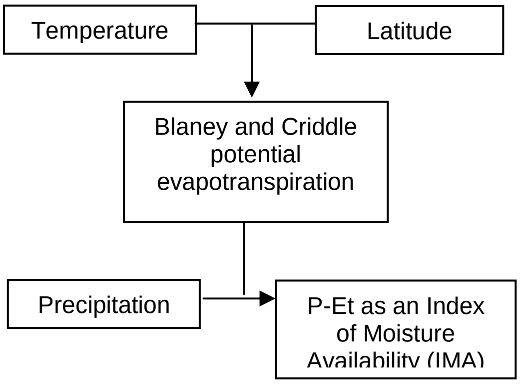

Figure 1 The procedure to calculate the IMA

3.3 The parent variables of the IMA

The IMA has three parent variables: temperature, precipitation and (calculated) potential evapotranspiration. We give examples in the following of the change in these variables between the control period, 1961-90 and the A2 scenario, 2071-2100, taking the example of the summer season. It should be noted that the B2 scenario generally shows changes which are less intense than those for the A2 scenario, but follow the same spatial patterns.

<u>Temperature</u>

The upper map of Figure 2 shows the change in mean temperature between the control and perturbed period for the A2 scenario. Summer temperatures increase by as much as 7°C, with the greatest change being seen over land gridboxes, especially north of the Mediterranean Sea. In the B2 scenario (not shown), the changes are around 2-3°C less.

Wnter A2 changes (not shown) are generally lower, in the range 2-3°C over the maritime fringe of western Europe and 5°C over the north-east of the study area. There is a less clear distinction between

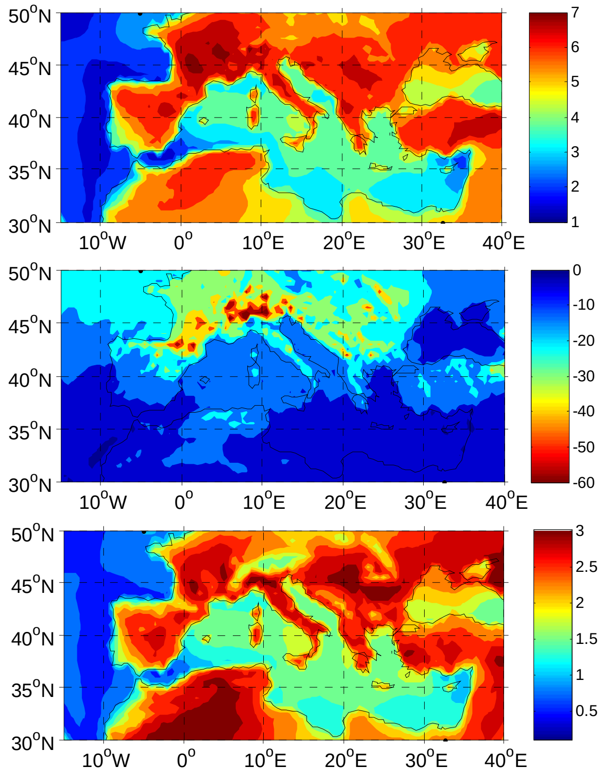

Figure 2. For the HadRM3 A2 scenario for summer, the change expressed as 2071-2100 – 1961-90 in: upper map mean temperature (°C); middle map average total rainfall (mm); lower map potential evapotranspiration (mm/day).

land and sea than was found in summer. The B2 scenario changes are around 2°C smaller.

<u>Precipitation</u>

Summer precipitation declines throughout the study region in the future A2 scenario. Small changes are seen over the Mediterranean Sea and land areas to the south, but it should be noted that rainfall amounts in summer are so low in this region that the capacity for a negative perturbation is small. To the north of the Mediterranean Sea, topography exerts a clear control over the precipitation perturbation, with largest negative changes (in the range -50 to -60 mm) over the Pyrenees and Alps. Again, it is likely that these high-altitude areas are picked out because their higher summer rainfall allows a greater potential for reduction. The changes in the B2 scenario (not shown) are very similar to those in the A2 scenario.

Winter precipitation changes (not shown) are not of a consistent sign in either the A2 or B2 scenario. For the A2 scenario, over the Mediterranean Sea and to the south precipitation is predicted to decline, with the largest differences, up to -40 mm, over sea areas. To the north-east and over the Alps, an increase in precipitation is predicted. The B2 scenario has a broadly similar spatial pattern, but the changes are smaller, rarely exceeding +/-20 mm.

Potential evapotranspiration

Summer ET shows a very clear land-sea contrast, although throughout the region the changes are positive in sign, indicating an increase in the 2070-2100 period. Over the land, the changes are everywhere in the range 2-3 mm/day, with the smallest amounts along the coastal margins and the largest values inland. Over the sea the changes are much lower, in the range 0-1.5 mm/day. The B2 scenario changes (not shown) have a similar spatial pattern, but are generally smaller.

The winter A2 patterns are quite different, with the whole region showing consistent increases of around 0.5-1 mm/day, slightly less in the B2 scenario.

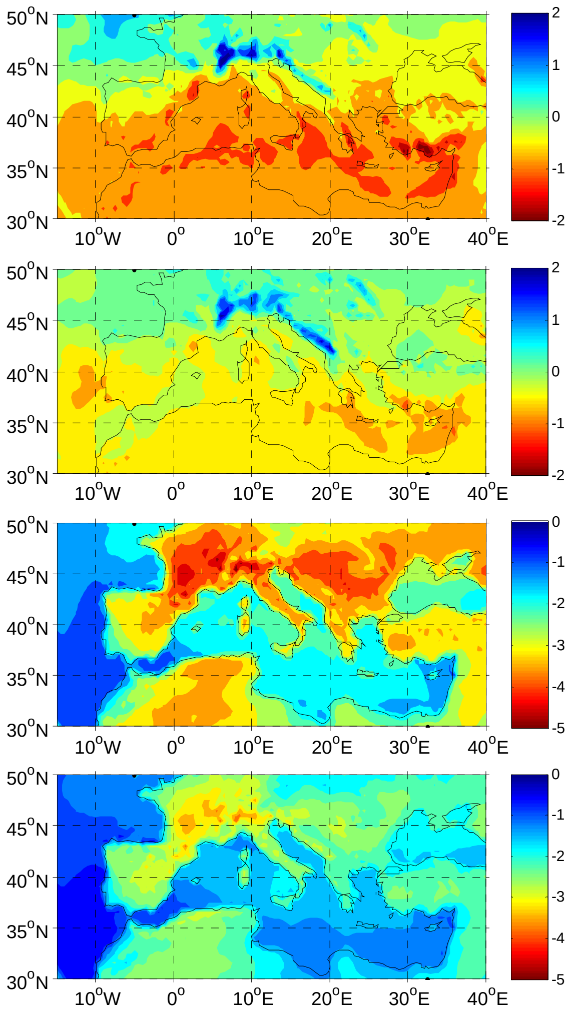

Figure 3. For HadRM3, the change expressed as 2071-2100 – 1961-90 in the IMA (mm/day). From the top, these show winter A2, winter B2, summer A2 and summer B2.

3.4 The IMA

Spatial patterns in the IMA

As noted, the IMA Is given by the difference, P – Et. Figure 3 shows, for winter and summer, IMA changes for the HadRM3 A2 and B2 scenarios in 2070-2100 compared to 1961-90. In winter there is a clear north-south contrast, with negative changes to the south and limited areas north of the Mediterranean Sea where positive changes are indicated. In the A2 scenario, the changes range between -2 mm/day in the south and, over mountainous areas to the north, +2 mm/day. The changes are smaller in the B2 scenario, generally between +/-1 mm/day, but again with larger positive changes over the Alps and the mountainous coast of ex-Yugoslavia. The altitudinal control in both scenarios is very clear.

In summer the changes are negative throughout the region in both the A2 and B2 scenarios, i.e., a reduction in moisture availability. Largest changes are seen over land areas to the north of the Mediterranean Sea. In the A2 scenario the reductions approach 5 mm/day in this area, whereas in the B2 scenario they are more typically 3-4 mm/day.

Inter-annual variability in the IMA

We can also inspect inter-annual variability in the IMA for selected gridboxes within the region. An example for Spain is shown in Figure 4. The upper figure shows the summer IMA for the present-day simulation of HAdRM3. The IMA is always negative, with a mean of around -4 mm/day and the lowest values not exceeding -6 mm/day. The lower figure shows the situation in 2070-2100, in which the IMA lies between -4 mm/day and -9 mm/day, with a mean of around -7 mm/day. Of note is the downward trend in the perturbed experiment. The wintertime perturbed scenario, by contrast, shows little difference compared to the present day, and contains no trend (not shown). Few differences between the different ensemble members are apparent in either season.

4. INDICES OF PRECIPITATION EXTREMES

The Mediterranean region experiences a long and persistent dry period throughout the summer months. If we search through the daily rainfall series of land-based grid points in HAdRM3 for the longest dry period in the year, then in the Mediterranean region this will fall in the summer months. We can explore the behaviour of this long summer drought by looking at changes in its length, its start and its end dates. These indices were calculated from daily HadRM3 data for the periods 1961-1990 and 2070-2100, for the SRES A2 and B2 scenarios, and the changes between the two periods used to further explore the potential impacts of global warming on the water resources of the Mediterranean Basin.

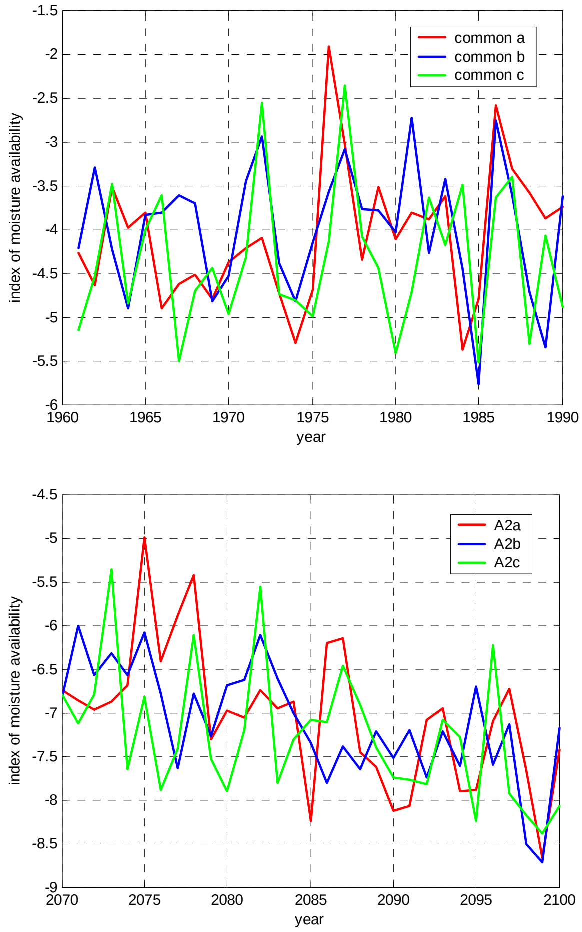

Figure 4. Summer IMA (mm/day) for a Spanish gridbox in HadRM3. Above: 1961-90. Below: 2070-2100

In Figure 5, we show the changes in these three measures, for the A2 scenario. The start date shows the greatest change over the central and south-eastern parts of the domain, occurring as much as 10-15 days earlier in the future scenario. Over much of Europe, and north-western Africa, there is little change. The end date for much of the area shows little change, or is slightly earlier. However, over the central and south-eastern area which showed an earlier start date in the upper map, a delay in the termination of the summer drought is indicated, by around 20 days. For this region, the behavior of the summer drought indicates a deterioration in the water resources situation in the 2070-2100 period. Elsewhere, the changes are smaller.

The lower map in Figure 4 shows the change in the length of the summer drought. As expected from the previous discussion, the summer drought is predicted to increase in length by about 15-30 days over the centre and south-east Mediterranean region in the A2 scenario, whilst becoming around 10 days shorter elsewhere. The spatial patterns in the B2 scenario are similar, but the change in the length of the summer drought is less, only around 10-20 days longer in the central and south-eastern Mediterranean, and close to zero over much of the remainder of the study area.

5. CONCLUSIONS

The IMA has the effect of integrating the separate changes in temperature and precipitation to give a more complete picture of the likely effects of climate change on water resources and hence human activities such as tourism and agriculture. The picture in the Mediterranean is one of little change in the winter season. The suggestion of positive changes in the IMA in winter over high altitude areas of Europe is of interest since this is likely to be manifest as changes in the snow pack, with beneficial implications for water storage and skiing. In summer, the indications are of large and widespread reductions in moisture availability, at a time when tourism, and hence demand for domestic water, is at its peak

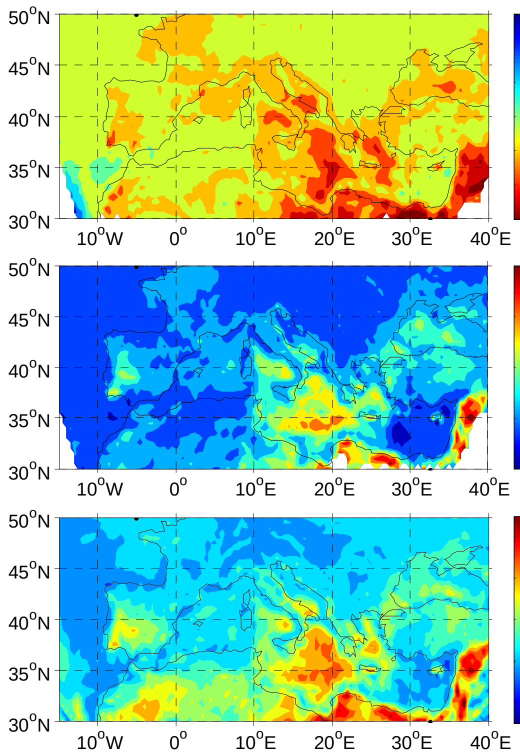

Figure 5. The change in precipitation indices expressed as the difference, 2070-2100 minus 1961-90. Upper map: start date of the drought. Middle map: end date of the drought. Lower map: length of the drought. Units, Julian days.

The IMA analysis demonstrated clearly that the greatest perturbation in moisture availability would be in the summer season. We therefore inspected the behaviour of the summer dry season, using only the information on precipitation from HadRM3. This analysis showed that, throughout the region south of the Mediterranean Sea, and to the north over much of central and southern Spain, southern Italy and Greece, the summer drought is predicted to lengthen by 2070-2100, by as much as 20-30 days in places, but more typically by around 10-15 days. This is due primarily to earlier onset rather than later cessation.

Overall, comparison of moisture availability between 1961-90 and 2070-2100 suggests little change in the winter season, or even some improvement over high altitude areas north of the Mediterranean Sea. In the summer, however, the situation is likely to deteriorate, suggesting that a reappraisal of water resource management is required, especially in the light of an anticipated rapid increase in tourist numbers.

ACKNOWLEDGEMENTS

This work was funded by the European Commission Framework Programme 5 under Contract EVK2-CT2001-00132 'Prediction of Regional scenarios and Uncertainties for Defining EuropeaN Climate change risks and Effects (PRUDENCE).

REFERENCES

Blaney, H.F., and Criddle, W.D., 1950: Determining water requirements in irrigated areas from climatological and irrigation data. *USDA (ARS) Technical Bulletin*, **1275**, 59 pp.

Dorrenbos, J., and Pruitt, W.O., 1977: Guidelines for predicting crop water requirements. *FAO Irrigation and Drainage Paper*, **24**, 144 pp.

European Environment Agency, 2001: *Indicator Fact Sheet Signals 2001 – Chapter Tourism*. Available from the web site: www.eea.eu.int.

Palutikof, J.P., Goodess, C.M. and Guo, X. 1994: Climate change, potential evapotranspiration and moisture availability in the Mediterranean Basin. *Int. J. Climatol* **14***,* 853-869.